Heliyon 8 (2022) e09148

Contents lists available at ScienceDirect

Heliyon

journal homepage: www.cell.com/heliyon

Research article

Microstructural and physicochemical properties of biodegradable films developed from false banana (*Ensete ventricosum*) starch

Buliyaminu A. Alimi [a,b,*], Tilahun S. Workneh [a], Bashir A. Zubair [b]

[a] *Bioresources Engineering, School of Engineering, College of Agriculture, Engineering and Science, University of KwaZulu-Natal, Private Bag X0l, Pietermaritzburg, Scottsville, 3209, South Africa*

[b] *Department of Food Science and Technology, School of Agriculture and Agricultural Technology, Federal University of Technology, P. M.B. 65, Minna, Nigeria*

ARTICLE INFO

Keywords:
Ensete
False banana
Biodegradable films
FTIR
Packaging

ABSTRACT

The recent trend in starch research is the exploration of potential applications of starches from under-utilized sources. Properties of edible biodegradable films developed from *ensete* 'false banana' (*Ensete ventricosum*) starch with glycerol as plasticizer were evaluated in this study. Microstructural examination revealed presence of pores which were gaining prominence with increasing glycerol content while FTIR analysis showed the presence of protein groups characteristic bands and existence of interactions between molecules (glycerol, starch, amide groups and water) in the polymerics. These revelations have profound effect on functional, mechanical and optical properties of the films. Thickness (156.70–189.00 μm), density (1.95–2.44 g/cm^3), swelling power (84.49–102.26%), water solubility (17.07–22.32%), water vapor permeability (1.40×10^{-8}-1.98×10^{-8} g/m s Pa), lightness 'l^*' (39.01–43.86) and energy difference (39.02–43.87) of the film were increasing with increasing glycerol content. The increase was significant ($p < 0.05$) with swelling power and water solubility, while puncture force (570.83–252.90 g) and film transparency (78.17–51.65%) decreased significantly ($p < 0.05$) with increasing glycerol content. X-ray diffraction revealed combination of C-type and processing induced V_H diffraction patterns. The results of this study exposed the promising potential of *ensete* starch for development of films and coatings for different packaging requirements.

1. Introduction

Until recently, the sole base material for plastic packaging films was synthetic polymers from petroleum. However, the continuous use of synthetic materials for plastic films food packaging is faced with some challenges. Principal concerns are the health safety of consumers due to presence of some high-risk compounds in synthetic plastics and environmental issues arising from their non-biodegradability (Shah et al., 2016). These have led to continuous research efforts to develop safe and eco-friendly plastic films. The most attractive replacements are macromolecules from renewable biological sources (Jafarzadeh et al., 2020). Biodegradation, renewability, comparative cheapness and human health safety are the principal appeals for the applications of films from biological materials in food and pharmaceutical sectors (Xue Mei et al., 2020; Alimi et al., 2021).

Films from biopolymers have been shown to enhance food quality and shelf-life, and may also be consumed along with the foods they cover (Daudt et al., 2016). Reports from different studies have further shown proteins and starch as important macromolecules, possessing great potentials, for the development of eco-friendly edible films (Daudt et al., 2016; Dai et al., 2019). Hence, Sustained production of films from agricultural biopolymers, as a value addition to agricultural products, would further enhance the income of farmers and other practitioners along the chain. However, starch is the most patronized base material for the fabrication of edible films because of its superior properties and excellent functionalities it imparted in the resulting films (Yıldırım-Yalçın et al., 2019).

Starch is receiving superior research attention because of its abundant availability, ease and high yield of extraction, low cost and array of functional properties which enhance its biocompatibility in food system (Shah et al., 2016; Pelissari et al., 2013). Edible films have been developed from several starch sources, which included corn, potato, banana and plantain, and their properties studied. The results had shown that morphological and physico-chemical properties of the source starch had significant influence on the final characteristics of the films (Daudt et al., 2016). Therefore, it is essential to study the final properties of edible film

* Corresponding author.
E-mail addresses: bun5574@yahoo.com, baalimi@gmail.com (B.A. Alimi).

https://doi.org/10.1016/j.heliyon.2022.e09148
Received 29 May 2021; Received in revised form 2 August 2021; Accepted 16 March 2022

from individual starch source to determine its strength and limitation. This is necessary for its adoption or otherwise in food packaging system.

Ensete (*Ensete ventricosum*, Musaceae) is a non-fruit bearing banana type plant (hence the name false banana) indigenous to Ethiopia. The plant has excellent adaptation to different climatic conditions. Besides being drought resistant, its ability to withstand low temperature makes it possible to be grown on highland. This is an edge it has over cassava (Gebre-Mariam et al., 1996) Its major economic value lies in the large reservoir of starch in its corms and pseudo stems (Alimi et al., 2016). *Ensete* starch was reported to contain minimal amount of impurities and hence could find great applications in the industry. *Ensete* belongs to the class of underutilized starch source because there is no report of the use of its starch for any industrial application. The major utilization of the starch is in the preparation of local delicacies consumed by people of the region (Gebre-Mariam et al., 1996). Developing edible films from it could be a value addition to its utilization and this could promote it as an important cash tree. Its successful utilization in edible film production would expand sources of starch for film making and reduce pressure on established starch sources. Consequently, this would enhance commercial utilization of *ensete* and improve the economy and livelihood of the practitioners along its value chains. Therefore, the aim of this work was to develop edible films from *ensete* starch and investigate their properties.

2. Materials and methods

2.1. Experimental materials

Ensete (*E. ventricosum*) starch was sourced from Knel Trading, South Africa. The starch was passed through 150 μm size sieve to ensure purity. Its moisture content was reduced from 20% to 12% by drying in a forced air convective oven for 24 h at 48 °C. Glycerol (1, 2, 3-propanetriol glycerin, G49776) was supplied by Sigma-Aldrich Pty Ltd, Johannesburg, South Africa.

2.2. Film preparation

Casting method described by Daudt et al. (2016) was modified to prepare edible films from the starch. Glycerol was added into suspension containing 3 g starch in 100 mL distilled water. The mixture was heated on hot plate at 85 °C with continuous magnetic stirring to eliminate bubbles and ensure uniform filmogenic solution. The heating and stirring continued until colorless and viscous liquid was formed (approximate time was 35 min). The film forming solutions (FFS) were left to cool, dispensed into uniform size circular acrylic non-sticky plate (30 g per plate for uniform thickness) and dried in an air circulation chamber under controlled temperature (40 °C) and humidity (50%) condition for 24 h. Developed Films were coded based on added glycerol (E1.5, E2.0 and E3.5, representing film containing 1.5, 2.0 and 3.5 mL glycerol, respectively). Dried films were carefully peeled from the plates, conditioned and hold at 58% relative humidity and 25 °C temperature in a controlled temperature and humidity chamber (CTS model C-40/100, Hechingen, GmbH) until analysis.

2.3. Microstructural analysis

Small fragments of the film samples obtained through fracturing with the aid of tweezers were mounted on stubs using double-sided tapes. Thin layer of gold was sputter-coated to the surface of the film using EIKO IB-3 sputter ion coater (EIKO Engineering, Hitachinaka, Japan). Microstructure of the films was captured using a scanning electron microscope (EVO LS 15, ZEISS International, Germany).

2.4. X-ray diffraction

Diffraction patterns of the film samples were captured with an X-ray diffractometer (D8 Advance, BRUKER AXS, Germany) at Bragg angle (2Θ) range of 3^o to 40^o, scan step of 0.035^o and step time of 0.5 s. Generator settings were 40 kV and 40 mA.

2.5. Infrared spectroscopy

A Fourier Transform Infrared (FTIR) spectrometer (Spectrum 100 series, PerkinElmer, Beaconsfield, UK) was used to obtain infrared spectra of the film samples. The analysis was conducted at wavelength range of 4000 to 380 cm^{-1} at spectra resolution of 4 cm^{-1} in the infrared region.

2.6. Thickness and density

Metric micrometer screw gauge 0–25 mm, 0.01 mm precision, was used to determine the thickness of the films taken at 5 random points in each of the film.

Film samples were cut into 30 × 30 mm^2 dimension and their weights were noted. Film density was determined as the ratio of weight per unit volume of the film.

2.7. Swelling power and water solubility

These were determined as described by Shittu et al. (2014). The initial dry mater of the film was first determined by drying 900 mm^2 of films in an oven at 100 °C for 24 h. The weight was noted and taken as F_o. The dried sample was then immersed in 25 mL distilled water contained in a beaker and left for 24 h under laboratory condition. The distilled water was filtered off and the squared film was carefully removed. Surface water was removed by blotting with non-shredding adsorbent paper. The new weight was recorded as F_1. The swelled film was then dried in an oven at 85 °C and regularly checked until constant weight F_2. Swelling power (SP) and water solubility (WS) were calculated as stated in Eqs. (1) and (2), respectively below.

$$SP = \left(\frac{F_1 - F_0}{F_0}\right) * 100 \quad (1)$$

$$WS = \left(\frac{F_0 - F_2}{F_0}\right) * 100 \quad (2)$$

2.8. Water vapor permeability

Desiccant method according to ASTM E96 was used to determine the water vapor permeability (WVP) of the studied films (Arezoo et al., 2020). Prior to the determination of WVP, all film samples were placed in desiccator containing silica gel (~0% relative humidity (rh)) for at least 5 days to equilibrate. Film samples were cut into circular sheet of 46 mm diameter, mounted and sealed using silicone on circular mouth glass cups containing dried silica gel. The weight of the assemblage was noted before placing in a desiccator. A 50 mL beaker filled with distilled water (~100% rh) at 30 °C was placed beside the assemblage in the desiccator. Weight gained was monitored periodically (every 1 h) until constant weight and the WVP was calculated using Eq. (3) below.

$$WVP = \frac{xh}{A\Delta P} \quad (3)$$

Where, x, is the gradient of weight gain over time (g/s), h, is the film thickness, A, is the surface area of the film (m^2), and ΔP is the vapor pressure difference across the film (Pa).

2.9. Film strength

The strength of the films was determined by conducting puncture test using a texture analyzer (TA.XT2, Stable Micro System Ltd, UK) as described by Pelissari et al. (2013). Film samples, cut into a disc of 30 mm

diameter, were mounted firmly unto a round capsule of 10 mm diameter. Cylindrical probe of 3 mm diameter moving perpendicularly to the film surface at a speed of 1 mm/s pierced through the film. The peak force obtained from force (g)/time (s) graph was taken as the puncture force.

2.10. Optical properties

The *Commission Internationale de l'Eclairage* (CIE) L^*, a^* and b^* color parameters were determined with the aid of a colorimeter (Chroma meter CR 400, Konica Minolta, Japan). Measurements were taken after standardizing the equipment with white tile provided by the manufacturer. Color difference, DE, was calculated as stated in Eq. (4).

$$DE = \sqrt{(L^2 + a^2 + b^2)} \quad 4$$

Light transmittance of the films was determined using a UV-visible spectrophotometer (UV/VIS Optima Scientific, South Africa) at 560 nm as described by Shittu et al. (2014). Film transparency (T_f) which was measured as light transmittance through the films was calculated according to Eq. (5)

$$T_f(\%) = 100^* \left(\frac{T_w}{T_o}\right) \quad 5$$

T_w is the light transmittance with the film, while T_o is the transmittance without the film.

2.11. Statistical analyses

Analyses were conducted at least in duplicates. One-way analysis of variance and Duncan Multiple Range Test (DMRT) in SPSS (15.0) environment were used to obtain and separate means at $p \leq 0.05$, respectively.

3. Results and discussion

3.1. Microstructure

Scanning electron microscope was used to observe possible changes in the structure of the films (Figure 1) at microscopic level. Pores observed on the surfaces of the films may be due to presence of non-starch macromolecules, such as protein, lipids and fiber, in the matricesThe presence of pores was reported for films made from starches from other sources such as pinhao (Daudt et al., 2016), and banana and plantain (Pelissari et al., 2013). . Traces of proteins and lipids in *ensete* starch were reported by Gebre-Mariam et al. (1996). Though it has been reported that these non-starch components are usually present in concentration lower than 5%, however, they play important roles in final film structure. These include interactions with amylopectin component of starch and between each other, leading to micro-segregation of phases (Daudt et al., 2016; Pelissari et al., 2013). The increase in prominence of the pores with increase in glycerol content could be due to hydrophobic effect of non-starch components (protein and lipids) which led to their self-aggregation and merging to form fiber-like structure (Liu et al., 2018). This phenomenon is important for the development of film with appropriate surface and barrier properties (Huntrakul et al., 2020).

3.2. X-ray diffraction

Variation in the degree of crystallinity of *ensete* starch films was observed with x-ray diffractometer. The diffraction patterns of the films are shown in Figure 2. Identified characteristic peaks at (2Θ) 5-6^o and 26^o (B type) and 16^o and 29^o (A type) suggested C-type crystallinity. Also, presence of peaks at 18^o and 22^o evidenced presence of processing induced V_H diffraction pattern (Alimi et al., 2017a,b). It is pertinent to mention that the characteristic pattern of native *ensete* starch is B-type crystal (Alimi et al., 2016; Gebre-Mariam et al., 1996). However, C-type crystallinity pattern was observed in this study for *ensete* starch films. Similar observation of diffraction pattern differences between source starch and films was also reported for potato starch and films (Mathew et al., 2006) and plantain banana starch and flour films (Pelissari et al., 2013).

3.3. Infrared spectroscopy

Possible variations that could occur in the chemical reactivity of *ensete* starch films were captured using FTIR spectroscope. There is no notable difference in the transmittance spectra of the films (Figure 3). Interactions at molecular level were identified through displacement or shift in intensity of assigned bands of the chemical groups (Ortega-Toro et al., 2016). The peak bands at 3262.70 to 3275.51 cm-^{1}were within the region of 3000–3600 cm^{-1} wavelength known for complex vibrational stretching of hydrogen bonded hydroxyl group (Yıldırım-Yalçın et al., 2019). Bands at 2885.08 (E2.5) to 2930.14 cm^{-1} (E1.5) were within the region (2800-3000 cm^{-1}) typical of CH bond stretching. The transmittance bands observed in the two regions were major carry-over from the starch structure (Mathew et al., 2006). The bands were due to the resultant effect of amylose/amylopectin content of starch (Pelissari et al., 2013).

Transmittance peak bands at 1647.36 (E2.0) to 1650.80 cm^{-1} (E1.5) were the effects of carbonyl bond stretching of amide I, while bands 1240.51 (E1.5) and 1234.33 cm^{-1} (E2.5) were in the region of amide III. Bands in amide III region were results of C–N bond stretching and N–H bonds inflexion. These bands are indication of the presence of residual proteins in the films. Bands in these regions were reported for plantain starch films (Pelissari et al., 2013), achira starch films (Andrade-Mahecha et al., 2012) and potato starch films (Mathew et al., 2006). Peaks at 1416.68 cm^{-1} (E1.5) and 1415.43 cm^{-1} (E2.5) are the typical O–C–O bond stretching which evidenced interaction between starch molecules and glycerol (Ortega-Toro et al., 2016).

The prominent bands observed at 1017.30 (E1.5) to 1019.95 cm^{-1} (E2.5) are due to the stretching of C–C, C–O and C–O–H bonds of starch (Pelissari et al., 2013).

Peak bands between 924 and 925 cm^{-1} were due to the contribution of saccharide structure. C–O, C–O–H and C–O–C bond stretching in the glycosidic backbone of starch are responsible for the bands (Arueya and Oyewale, 2015). Alimi and Workneh (2018) reported that the presence of

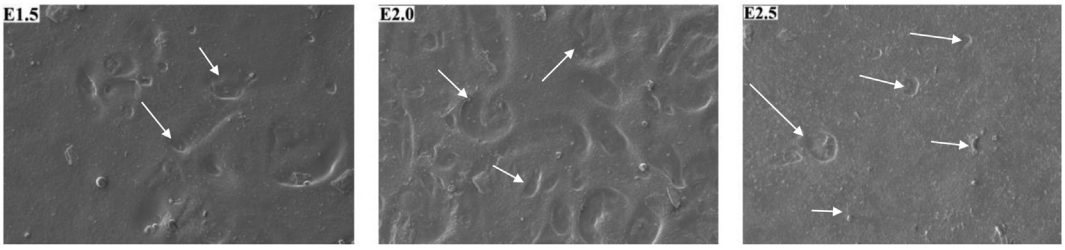

Figure 1. Scanning electron micrograph of surfaces of *ensete* starch films based on: (E1.5) 1.5 mL glycerol in film forming solution, (E2.0) 2.0 mL glycerol in film forming solution, (E2.5) 2.5 mL glycerol in film forming solution at 500x magnification.

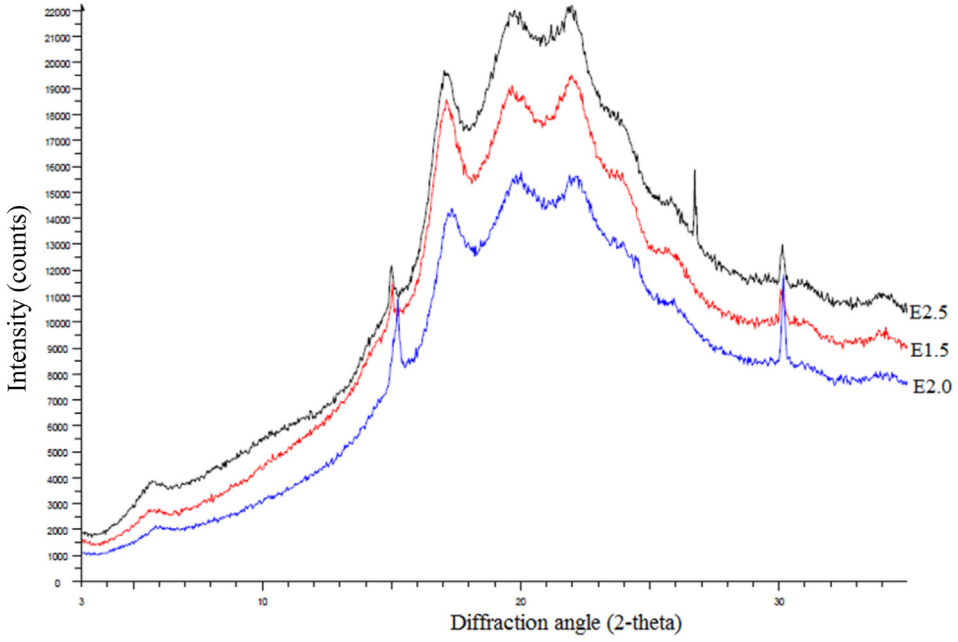

Figure 2. X-ray diffraction patterns of *ensete* starch films based on: (E1.5) 1.5 mL glycerol in film forming solution, (E2.0) 2.0 mL glycerol in film forming solution, (E2.5) 2.5 mL glycerol in film forming solution.

α-1,6 glycosidic bonds of amylopectin may be responsible for the differences in the location and intensity of the bands.

3.4. Thickness and density

Increasing addition of glycerol did not have statistically significant ($p < 0.05$) effect on thickness of the films (Table 1). This could be due to the fact that the major factor, which is the ratio of dry matter to surface area, controlling the final thickness of films are fixed (The et al., 2009). Same quantity of film forming solutions were dispensed into uniform dimensioned petri dishes. Müller, Yamashita and Laurindo (Müller et al., 2008) also reported that amount of plasticizer did not significantly affect the thickness of films made from cassava starch. Control of thickness of film is an important processing step during film preparation because of its effect on barrier of films to water vapor pressure and gases (Gutiérrez et al., 2015).

Density of the films increased, though not statistically significant ($P > 0.05$), from 19.46 (E1.5) to 24.37 (E2.5) with increase in glycerol content. Daudt et al. (2016) also observed insignificant difference in density of films made from the same base materials.

3.5. Swelling power and water solubility

Swelling power of a biopolymer is an indication of its hydration capacity (Alimi et al., 2017a,b). Swelling power of the films was found to be increasing with glycerol content (Table 1). The increase was significant ($p < 0.05$) at 2.5 mL glycerol in 100 mL FFS. The increase in swelling power of the films with increase in plasticizer content could be the result of structural re-alignment within the film (Alimi et al., 2016). Continuous addition of glycerol could have resulted in the weakening of interactive forces within the film matrices. The reduction in internal cohesion of film matrix enhanced the movement of ions in the film, thereby altering the osmotic pressure and resulting into swelling occasioned by water transfer into the matrix (Mathew et al., 2006). Since SP is an indication of the ability of the film to conserve the quality of wrapped materials during holding and storage (Nouraddini et al., 2018), film swelling will be a beneficial attribute for biomedical application because of the enhancement of absorption of water and bioactive compounds by the film without it being dissolved and subsequently ensuring slow release of drug thereby reducing molecular diffusion.

Solubility of the films in water followed similar trend with SP (Table 1). The values ranged from 17.07 to 22.32 g/100 g. The hygroscopic nature of glycerol was reported to be responsible for the increase in water solubility of films with increasing addition of glycerol. It is worth mentioning that films maintained their integrity throughout the solubility experimental period. This good attribute, which was similarly reported by Pająk et al., 2019, could propel the use of *ensete* starch films for fruits and drug wrapping especially for holding coated products in high water activity environment or to avoid exudation of fresh or frozen materials when in contact with water.

The desired value range for film solubility in water is dependent on its intended application. The values obtained in this study are neither high nor low but in the moderate course range comparable to value of 21.3 g/100 g reported for banana starch film with 19 g glycerol in 100g starch (Pelissari et al., 2013). Some other values reported in the literature are 28.4 g/100g for achira starch films containing 17. g glycerol in 100. g starch (Mathew et al., 2006) and 62.50 g/100g for amaranth starch film containing 22.50 g glycerol in 100.00 g starch (Müller et al., 2008).

3.6. Water vapor permeability

Permeability property of films is important when considering the suitability of films for specific packaging requirement, especially, when control over environment conditions is of top priority. There was no significant difference in water vapor permeability of the films (Table 1). This showed that increase in glycerol content was not enough to allow greater ease of water movement through the films. Presence of hydrophobic non-starch components in the films, strong interactive forces within the film matrices and possible twisting structure of the films which hinder water diffusion (Pelissari et al., 2013) may be responsible for this observation. The sustained structural integrity further confirm *ensete* starch films as good candidates for packaging in a damp environment.

3.7. Film strength

Maximum force required for the test probe to pierce through the films was taken as a measure of the strength of the films. It is an indication of

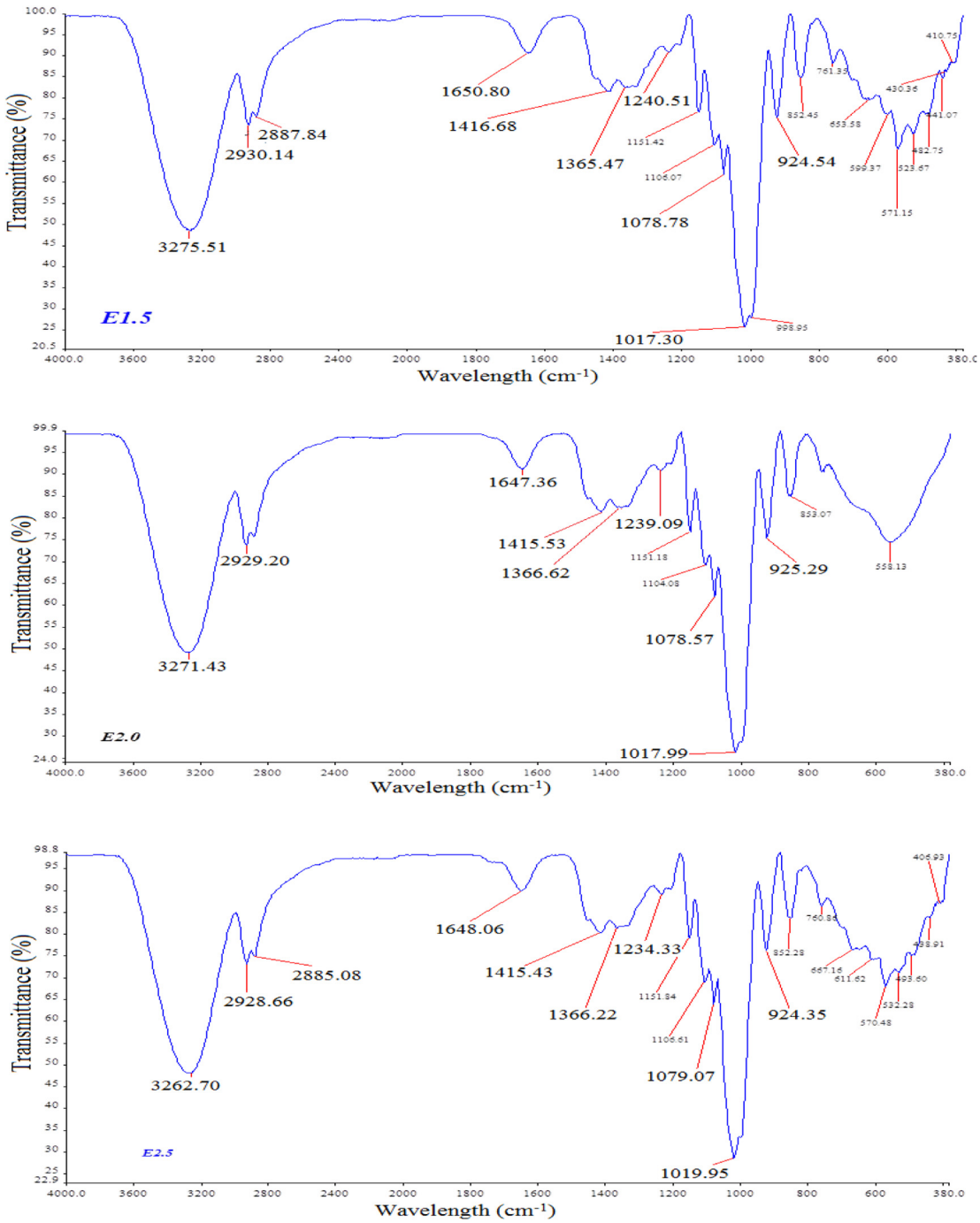

Figure 3. FTIR spectra of *ensete* starch films based on: (E1.5) 1.5 mL glycerol in film forming solution, (E2.0) 2.0 mL glycerol in film forming solution, (E2.5) 2.5 mL glycerol in film forming solution.

the resistance of films to puncturing. Strength of *ensete* starch films as indicated by the puncture force is shown in Table 1. Strength of the films was decreasing (570.83–252.90 g) significantly ($p < 0.05$) with increasing content of glycerol in FFS. Variation in the film strength with glycerol content is an indication of structural changes that occurred due to increasing plasticizing effect of continuous addition of glycerol. The trend is well known and has been reported by several authors (Mousavian et al., 2021; Akman et al., 2021). Like other plasticizers, glycerol act by limiting interaction and proximity between starch chains thus facilitating mobility within the matrix and enhancing flexibility (Mousavian et al., 2021). It has been reported that plasticizers do not act singly to reduce the cohesive force in the starch matrix in films. Moisture and presence of some impurities such as lipid and protein were reported to enhance the plasticizing effect of glycerol (Gutiérrez et al., 2015). Increasing glycerol content implied more moisture absorption due to its hygroscopic nature and this leads to further weakening of interactive forces within the polymer matrix. This resulted in reduction in mechanical resistance and increasing flexibility of biopolymer films (Godbillot et al., 2006).

The force-time curves of the films generally show non-linear increase of force with distance until breaking point (Figure 4) *Ensete* starch films with 1.5% glycerol content showed more rigidity and this was decreasing with increasing glycerol content. The trend was similarly reported by Gutiérrez et al. (2015) for cush-cush yam and cassava starch films, and Pelissari et al. (2013) for banana starch and flour films.

Table 1. Functional and mechanical properties of *ensete* starch films.

Sample	Thickness (μm)	Density (g/cm^3)	SP (%)	WS (%)	WVP (10^{-8} g/m s Pa)	Puncture force (N)
E1.5	156.70^a ± 0.58	1.946^a ± 0.51	84.49^a ± 1.61	17.07^a ± 0.39	1.769^a ± 0.743	5.59^b ± 0.85
E2.0	168.30^a ± 0.76	2.347^a ± 0.12	88.95^a ± 3.52	18.92^a ± 1.29	1.911^a ± 0.751	3.34^a ± 0.96
E2.5	189.00^a ± 3.44	2.437^a ± 0.48	102.26^b ± 8.28	22.32^b ± 3.29	1.977^a ± 0.502	2.48^a ± 0.33

Mean ± SD. Mean with different superscript letters along a column are significantly different ($p < 0.05$). Experiments were done in triplicate. One-way analysis of variance and Duncan Multiple Range Test (DMRT) in SPSS (15.0) environment were used to obtain and separate means at $p \leq 0.05$, respectively.
E1.5: Film containing 1.5 mL glycerol; E2.0: Film containing 2.0 mL glycerol; E2.5: Film containing 2.5 mL glycerol; SP: Swelling power, WS: Water solubility; WVP: water vapor permeability.

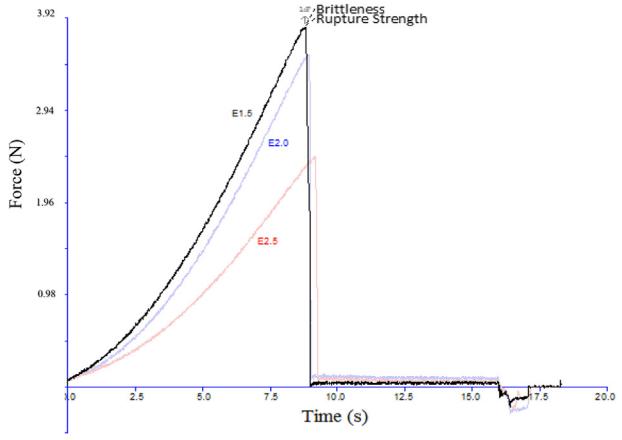

Figure 4. Force-time curves showing puncture force of *ensete* starch films based on: (E1.5) 1.5 mL glycerol in film forming solution, (E2.0) 2.0 mL glycerol in film forming solution, (E2.5) 2.5 mL glycerol in film forming solution.

Puncture force of the films is a measure of the flexibility of the films (Pelissari et al., 2013). High puncture force indicates low flexibility. Mechanical strength requirement of plastic films depends on its intending end use. Edible biodegradable films for fruits and food wrapping require high flexibility which could be found in E2.5, while the requirement for packaging material to reinforce food structure is rigidity and great resistance to deformation and this could be found in E1.5.

3.8. Optical properties

Color is responsible for visual appearance as perceived by consumers. Visual appearance of a product is an important determinant of its acceptability by consumer (Alimi et al., 2014). Increasing glycerol content did not have statistically significant ($p < 0.05$) effect on primary and secondary color parameters studied (Table 2). Except *b*, values of other parameters were increasing with glycerol content. It is important to mention that all films were lighter in color as evidenced by their *l* values (Gutiérrez et al., 2015). Aside *ensete* starch film with 1.5 mL glycerol content which showed slight tinge of magenta, others indicated tendency to green color as shown with their positive *a* values. The general positive *b* values indicated yellowish coloration. With this, we can conveniently infer that *ensete* starch films showed high tendency to light greenish-yellow coloration. Increasing glycerol content did not have significant ($p < 0.05$) on color difference, *DE*, of the films. The implication is the uniformity in color of the films within the studied glycerol range.

Glycerol content had significant ($p < 0.05$) effect on transparency of the films. Transparency of the films was reducing progressively from 78.17 (E15) to 51.65% (E2.5) with increasing glycerol content (Table 2). Desired film transparency level is determined by the products to be coated or protected. Highly transparent film is needed for shelf display of some products to expose their aesthetic and enhance their acceptance by consumers. Conversely, an opaque or film of medium to low transparency, such as E2.5, may be required to wrap light sensitive products (Shittu et al., 2014).

Optical properties of films are determined by their constituent materials. Presence of impurities such as lipids and proteins in starch used for film making have been reported to be responsible for yellow tone and level of opacity observed for some films (Pelissari et al., 2013; Akman et al., 2021).

4. Conclusions

The results obtained from this study showed *ensete* starch as a promising candidate for the development of edible films for varying food and pharmaceutical applications. Structural analysis indicated that the starch films exhibited compact and cohesive structure. Pores observed on the surfaces of the films suggested presence of non-starch components like protein, lipids and fiber in the film matrices. Transmission peak bands observed in the regions of amide I and III, with the aid of FTIR spectroscope, further indicated the presence of residual proteins in the films. Molecular interactions within the polymeric were also captured. The films showed C-type and processing induced V_H diffraction patterns. These findings had major influence on the studied properties of the films. The swelling attribute of the films without being dissolved in water could promote them for biomedical application where slow drug release is desired. The sustained structural integrity as confirmed with water vapor permeability study showed *ensete* starch films as good candidates for packaging in damp environment. High transparency shown by *ensete* film with the lowest glycerol content (E1.5) could present it as a good packaging material to expose the aesthetic and enhance the acceptance of some products to consumers. Examples include freshly consumed fruits

Table 2. Optical properties of *ensete* starch films.

Sample	*l*	*a*	*b*	*DE*	T_f (%)
E1.5	39.01 ± 0.39	-0.02 ± 0.02	0.86 ± 0.31	39.02 ± 0.38	78.17^b ± 2.87
E2.0	42.92 ± 1.74	0.02 ± 0.02	1.02 ± 0.28	4293 ± 1.75	57.50^a ± 4.83
E2.5	43.86 ± 6.34	0.40 ± 0.04	0.73 ± 0.49	43.87 ± 6.34	51.65^a ± 2.28

Mean ± SD. Mean with different superscript letters along a column are significantly different ($p < 0.05$). Except T_f which was repeated thrice, other experiments were done in duplicate. One-way analysis of variance and Duncan Multiple Range Test (DMRT) in SPSS (15.0) environment were used to obtain and separate means at $p \leq 0.05$, respectively.
E1.5: Film containing 1.5 mL glycerol; E2.0: Film containing 2.0 mL glycerol; E2.5: Film containing 2.5 mL glycerol; *l*: Lightness index; *a*: Red-green index; *b*: Yellow-blue index; *DE*: Color difference; *Tf*: Film transparency.

and rolls. Whereas film with high glycerol content (E2.5) could be used to wrap light sensitive products. Results of this study have exposed ensete starch as a budding material for fabrication of films for different packaging and coating end uses in the food and pharmaceutical sectors. The successful commercial utilization of films from ensete starch will improve the economy and livelihood of the stakeholders along its value chains.

5. Data transparency

Research data are available.

6. Code availability

Not applicable.

Declarations

Author contribution statement

Buliyaminu A. Alimi: Conceived and designed the experiments; Performed the experiments; Analyzed and interpreted the data; Contributed reagents, materials, analysis tools or data; Wrote the paper.

Tilahun S. Workneh: Conceived and designed the experiments; Contributed reagents, materials, analysis tools or data; Wrote the paper.

Bashir A. Zubair: Analyzed and interpreted the data; Wrote the paper.

Funding statement

This work was supported by the University of KwaZulu-Natal, South Africa. Dr. Buliyaminu Adegbemiro Alimi was supported by the College of Agriculture, Engineering and Sciences, University of KwaZulu-Natal, South Africa (postdoctoral fellowship award).

Data availability statement

Data will be made available on request.

Declaration of interests statement

The authors declare no conflict of interest.

Additional information

No additional information is available for this paper.

References

Akman, P.K., Bozkurt, F., Dogan, K., Tornuk, F., Tamturk, F., 2021. Fabrication and characterization of probiotic Lactobacillus plantarum loaded sodium alginate edible films. J. Food Meas. Charact. 15 (1), 84–92.

Alimi, B.A., Shittu, T.A., Sanni, L.O., 2014. Effect of hydrocolloids and egg content on sensory quality of coated fried yam chips. J. Culin. Sci. Technol. 12 (2), 168–180.

Alimi, B.A., Workneh, T.S., Sibomana, M.S., 2016. Effect of hydrothermal modifications on functional, pasting and structural properties of false banana (Ensete ventricosum) starch. Food Biophys. 11 (3), 248–256.

Alimi, B.A., Sibomana, M.S., Workneh, T.S., Oke, M.O., 2017a. Some engineering properties of composite corn-banana custard flour. J. Food Process. Eng. 40 (3), e12444.

Alimi, B.A., Workneh, T.S., Oyeyinka, S.A., 2017b. Structural, rheological and in-vitro digestibility properties of composite corn-banana starch custard paste. LWT Food Sci. Technol. 79, 84–91.

Alimi, B.A., Workneh, T.S., 2018. Structural and physicochemical properties of heat moisture treated and citric acid modified acha and iburu starches. Food Hydrocolloids 81, 449–455.

Alimi, B.A., Workneh, T.S., Femi, F.A., 2021. Fabrication and characterization of edible films from acha (Digitalia exilis) and iburu (Digitalia iburua) starches. CyTA - J. Food 19 (1), 493–500.

Andrade-Mahecha, M.M., Tapia-Blácido, D.R., Menegalli, F.C., 2012. Development and optimization of biodegradable films based on achira flour. Carbohydr. Polym. 88 (2), 449–458.

Arezoo, E., Mohammadreza, E., Maryam, M., Abdorreza, M.N., 2020. The synergistic effects of cinnamon essential oil and nano TiO2 on antimicrobial and functional properties of sago starch films. Int. J. Biol. Macromol. 157, 743–751.

Arueya, G.L., Oyewale, T.M., 2015. Effect of varying degrees of succinylation on the functional and morphological properties of starch from acha (Digitaria exilis Kippis Stapf). Food Chem. 177, 258–266.

Dai, L., Zhang, J., Cheng, F., 2019. Effects of starches from different botanical sources and modification methods on physicochemical properties of starch-based edible films. Int. J. Biol. Macromol. 132, 897–905.

Daudt, R.M., Avena-Bustillos, R.J., William<s, T., Wood, D.F., Külkamp-Guerreiro, I.C., Marczak, L.D.F., McHugh, T.H., 2016. Comparative study on properties of edible films based on pinhão (Araucaria angustifolia) starch and flour. Food Hydrocolloids 60, 279–287.

Gebre-Mariam, T., Abeba, A., Schmidt, P.C., 1996. Isolation and physico-chemical properties of enset starch. Starch Staerke 48 (6), 208–214.

Godbillot, L., Dole, Patrice, Joly, Catherine, Rogé, Barbara, Mathlouthi, Mohamed, 2006. Analysis of water binding in starch plasticized films. Food Chem. 96 (3), 380–386.

Gutiérrez, T.J., Tapia, M.S., Pérez, E., Famá, L., 2015. Structural and mechanical properties of edible films made from native and modified cush-cush yam and cassava starch. Food Hydrocolloids 45, 211–217.

Huntrakul, K., Yoksan, R., Sane, A., Harnkarnsujarit, N., 2020. Effects of pea protein on properties of cassava starch edible films produced by blown-film extrusion for oil packaging. Food Pack. Shelf Life 24, 100480.

Jafarzadeh, S., Jafari, S.M., Salehabadi, A., Nafchi, A.M., Kumar, U.S.U., Khalil, H.A., 2020. Biodegradable green packaging with antimicrobial functions based on the bioactive compounds from tropical plants and their by-products. Trends Food Sci. Technol. 100, 262–277.

Liu, X., Yang, Y.J., Wang, Z.W., 2018. Structure characteristics of Coix seeds prolamins and physicochemical and mechanical properties of their films. J. Cereal. Sci. 79, 233–239.

Mathew, S., Brahmakumar, M., Abraham, T.E., 2006. Microstructural imaging and characterization of the mechanical, chemical, thermal, and swelling properties of starch–chitosan blend films. Biopolymers: Orig. Res. Biomol. 82 (2), 176–187.

Mousavian, D., Nafchi, A.M., Nouri, L., Abedinia, A., 2021. Physicomechanical properties, release kinetics, and antimicrobial activity of activated low-density polyethylene and orientated polypropylene films by Thyme essential oil active component. J. Food Meas. Charact. 15 (1), 883–891.

Müller, C.M., Yamashita, F., Laurindo, J.B., 2008. Evaluation of the effects of glycerol and sorbitol concentration and water activity on the water barrier properties of cassava starch films through a solubility approach. Carbohydr. Polym. 72 (1), 82–87.

Nouraddini, M., Esmaiili, M., Mohtarami, F., 2018. Development and characterization of edible films based on eggplant flour and corn starch. Int. J. Biol. Macromol. 120, 1639–1645.

Ortega-Toro, R., Muñoz, A., Talens, P., Chiralt, A., 2016. Improvement of properties of glycerol plasticized starch films by blending with a low ratio of polycaprolactone and/or polyethylene glycol. Food Hydrocolloids 56, 9–19.

Pająk, P., Przetaczek-Rożnowska, I., Juszczak, L., 2019. Development and physicochemical, thermal and mechanical properties of edible films based on pumpkin, lentil and quinoa starches. Int. J. Biol. Macromol. 138, 441–449.

Pelissari, F.M., Andrade-Mahecha, M.M., do Amaral Sobral, P.J., Menegalli, F.C., 2013. Comparative study on the properties of flour and starch films of plantain bananas (Musa paradisiaca). Food Hydrocolloids 30 (2), 681–690.

Shah, U., Naqash, F., Gani, A., Masoodi, F.A., 2016. Art and science behind modified starch edible films and coatings: a review. Compr. Rev. Food Sci. Food Saf. 15 (3), 568–580.

Shittu, T.A., Jayaramudu, J., Sivakumar, D., Sadiku, E.R., 2014. Physicochemical and engineering properties of nanocomposite films based on chitosan and pseudoboehmite alumina. Food Bioprocess Technol. 7 (8), 2423–2433.

The, D.P., Debeaufort, F., Voilley, A., Luu, D., 2009. Biopolymer interactions affect the functional properties of edible films based on agar, cassava starch and arabinoxylan blends. J. Food Eng. 90 (4), 548–558.

Xue Mei, L., Mohammadi Nafchi, A., Ghasemipour, F., Mat Easa, A., Jafarzadeh, S., Al-Hassan, A.A., 2020. Characterization of pH sensitive sago starch films enriched with anthocyanin-rich torch ginger extract. Int. J. Biol. Macromol. 164, 4603–4612.

Yıldırım-Yalçın, M., Şeker, M., Sadıkoğlu, H., 2019. Development and characterization of edible films based on modified corn starch and grape juice. Food Chem. 292, 6–13.